Author Manuscript

Author Manuscript

Author Manuscript

Author Manuscript

HHS Public Access

Author manuscript

*Lung Cancer*. Author manuscript; available in PMC 2016 November 01.

Published in final edited form as:

*Lung Cancer*. 2015 November ; 90(2): 321–325. doi:10.1016/j.lungcan.2015.09.018.

# From genotype to phenotype: Are there imaging characteristics associated with lung adenocarcinomas harboring RET and ROS1 rearrangements?

**Andrew J Plodkowski, MD**[1], **Alexander Drilon, MD**[2], **Darragh F Halpenny, MD**[1], **Dearbhail O'Driscoll, MB Bch, BAO**[1], **Donald Blair, MD**[1], **Anya M. Litvak, MD**[2], **Junting Zheng, MS**[3], **Chaya S Moskowitz, PhD**[3], and **Michelle S Ginsberg, MD**[1]

Andrew J Plodkowski: plodkowa@mskcc.org; Alexander Drilon: DrilonA@mskcc.org; Darragh F Halpenny: halpennd@mskcc.org; Dearbhail O'Driscoll: dearbhailodriscoll@gmail.com; Donald Blair: djblair73@yahoo.com; Anya M. Litvak: alitvak@gmail.com; Junting Zheng: ZhengJ@mskcc.org; Chaya S Moskowitz: moskowc1@mskcc.org; Michelle S Ginsberg: ginsberm@mskcc.org

[1]Department of Radiology, Memorial Sloan-Kettering Cancer Center, 1275 York Avenue, New York, NY 10065 USA

[2]Thoracic Oncology Service, Division of Solid Tumor Oncology, Department of Medicine, Memorial Sloan-Kettering Cancer Center, 1275 York Avenue, New York, NY 10065 USA

[3]Department of Epidemiology and Biostatistics, Memorial Sloan-Kettering Cancer Center, 1275 York Avenue, New York, NY 10065 USA

## Abstract

**INTRODUCTION—**Recurrent gene rearrangements are important drivers of oncogenesis in non-small cell lung cancers. *RET* and *ROS1* rearrangements are each found in 1–2% of lung adenocarcinomas and represent distinct molecular subsets. This study assessed the computed tomography (CT) imaging features of patients with *RET*- and *ROS1*-rearranged lung cancers.

**METHODS—**Eligible patients included pathologically-confirmed lung adenocarcinomas of any stage with a *RET* or *ROS1* rearrangement via fluorescence in-situ hybridization or next-generation sequencing, and available pre-treatment baseline imaging for review. A cohort of *EGFR*-mutant lung cancers was identified as a control group. CT features assessed included location, consistency, contour, presence of cavitation, and calcification of the primary tumor. Presence of an effusion, lung metastases, adenopathy and extrathoracic disease were recorded. The Wilcoxon rank-sum/Kruskal-Wallis and Fisher's exact tests were used to compare features between groups.

**RESULTS—**73 patients with lung adenocarcinomas were identified: 17 (23%) with *ROS1* fusions, 25 (34%) with *RET* fusions and 31 (43%) with *EGFR* mutations. *ROS1*-rearranged lung

**Address for correspondence**: Dr. Andrew Plodkowski, Department of Radiology, Memorial Sloan-Kettering Cancer Center, 1275 York Ave, New York, NY 10065, Phone: 646-888-5458, Fax: 646-888-4912, plodkowa@MSKCC.ORG.

**Publisher's Disclaimer:** This is a PDF file of an unedited manuscript that has been accepted for publication. As a service to our customers we are providing this early version of the manuscript. The manuscript will undergo copyediting, typesetting, and review of the resulting proof before it is published in its final citable form. Please note that during the production process errors may be discovered which could affect the content, and all legal disclaimers that apply to the journal pertain.

**Conflict of interest:**
The authors have no conflict of interest to declare.

Author Manuscript Author Manuscript Author Manuscript Author Manuscript

cancers were more likely to present as peripheral tumors in comparison to *EGFR*-mutant lung cancers (32% vs 65%, p=0.04). *RET*-rearranged lung cancers did not significantly differ from *EGFR*-mutant lung cancers radiographically. The consistency of the primary lesion for *RET* and *ROS* fusions and EGFR mutations were most frequently solid and spiculated.

**CONCLUSIONS—**Lung adenocarcinomas with *RET* and *ROS1* fusions share many radiographic features and those with ROS1 fusion are more likely to present as peripheral lesions in comparison to *EGFR*-mutant lung cancers.

### Keywords

Lung Adenocarcinoma; Computed Tomography; ROS1 Rearrangement; RET Rearrangement; EGFR Mutation

## 1. Introduction

Lung cancer is the leading cause of death among both men and women in the United States. In 2015, 221,220 new cases of lung cancer are expected with an estimated 158,040 deaths. [1] Non-small cell lung cancer (NSCLC) accounts for approximately 85% of these cases.[1] In recent years, the discovery of somatic genomic alterations in driver oncogenes has lead to better understanding in the development and treatment of lung cancers. In 2004, the discovery of the *EGFR* mutation in tumors from patients with lung adenocarcinomas who responded dramatically to targeted EGFR tyrosine kinase inhibitors ushered in an era of molecularly targeted therapy. [2–4]

Most recently, chromosomal rearrangements involving *ALK, ROS1,* and *RET* have been identified as targetable drivers of lung adenocarcinomas [5]. These rearrangements lead to the formation of chimeric fusion kinases that drive downstream growth pathway signaling and cellular growth and proliferation. *ALK*, *ROS1*, and *RET* rearrangements are associated with specific clinicopathologic features including a history of never or former light smoking, younger age, and adenocarcinoma histology [6]. These genomic alterations are mutually exclusive with other oncogenic drivers such as *EGFR* and *KRAS* mutations.

Radiogenomics has become of recent clinical interest and has specifically been used in lung cancer to characterize the radiological appearance of tumors harboring specific driver oncogenes. *ALK*-rearranged lung adenocarcinomas are associated with larger volume tumors, multifocal thoracic lymphadenopathy, and lymphangitic metastasis. [7, 8]

To our knowledge, there have been no reports describing the radiologic features of lung adenocarcinomas harboring *RET* or *ROS1* rearrangements. The goal of this study was to describe the CT features of tumors harboring these rearrangements, and to attempt to identify any differentiating characteristics in comparison to *EGFR*–mutant lung adenocarcinomas.

Author Manuscript Author Manuscript Author Manuscript Author Manuscript

## 2. Materials and Methods

### 2.1 Patient Cohort

Our institutional review board approved and waived the informed consent for this retrospective study. Patients with pathologically-confirmed lung adenocarcinoma of any stage harboring, *ROS1*, or *RET* fusions were identified from a prospectively maintained database of patients presenting to the thoracic oncology clinic at our institution between October 2007 and September 2014. Molecular profiling for these alterations was performed either via break apart fluorescence in situ hybridization (FISH) or broad, hybrid-capture next-generation sequencing (MSK-IMPACT, Illumina HiSeq). Patients without available CT images on the institutional Picture Archiving and Communication System (PACS, GE Centricity RA100) were excluded from the study. As a control group, a cohort of 31 patients harboring an *EGFR* mutation was selected from a separate institutional database. Clinical information collected on each patient from the institution's electronic medical record included age, sex and stage of disease.

### 2.2 Image Analysis

The earliest available CT before treatment was selected for image analysis. Each CT was reviewed in consensus by 2 of 4 radiologists with one consistent reader as the senior radiologist (D.B., D.O., A.P., and M.G. with 5, 5, 7, and 23 years of radiology experience respectively). The readers were blinded to the molecular profiling status of the patient, and all clinical details at the time of image interpretation. All images were reviewed on the institutional PACS system. The imaging protocol for each CT varied given 54 (74%) patients had imaging from an outside institution given the large number of cancer referrals to our center. CT slice thickness varied from 1.25mm to 5mm. 44 (61%) of the CTs were performed with intravenous (IV) contrast, while 29 (40%) were without contrast and performed on either a 16 or 64 slice CT scanner.

**2.2.1 Characteristics of the primary tumor—**The size of the primary tumor was defined on lung windows by measuring the longest axis for the length and then taking the longest perpendicular distance to determine the width.[9] The location of the primary tumor was determined to be central or peripheral. Central was defined as any lesion contacting a central bronchus to the lobar level; any lesion beyond this level was defined as peripheral.

The contour of the primary tumor was recorded as round (sphere with clearly defined smooth margins), lobulated (not spherical with clearly defined smooth margins), spiculated (solid lesion with linear extensions into the adjacent lung parenchyma) or consolidation (ill defined mass with the appearance of pneumonia).

The consistency of the primary tumor was recorded as solid (density obscures underlying pulmonary vessels and parenchyma), ground glass (increased attenuation of the lung parenchyma with preserved visualization of the underlying pulmonary vessels), mixed (containing both components of ground glass and solid characteristics), and air bronchograms (persistent visualization of the bronchi with surrounding increased

Author Manuscript Author Manuscript Author Manuscript Author Manuscript

attenuation). Additional characteristics of cavitation (pockets of air within the lesion) and calcification (any part of the lesion exceeding 100 Hounsfield units) were recorded.

**2.2.2 Ancillary features—**Associated findings to the primary tumor that were recorded were the presence of lymphadenopathy and volume (nodes measuring between ≥1cm and <1.5cm, ≥1.5 and <3cm, or ≥3cm in short axis); pleural effusion size (large or small) and laterality; lung metastases (additional lung parenchyma neoplasms) and extrathoracic disease (metastatic disease presence and location).

### 2.3 Statistical Analysis

The Wilcoxon rank-sum/Kruskal-Wallis tests and Fisher's exact test were used to compare continuous characteristics (age, size) and categorical features, respectively, between groups.

## 3. Results

### 3.1 Patient characteristics

Seventeen patients with lung adenocarcinomas harboring *ROS1* fusions and 25 patients with lung adenocarcinomas harboring the *RET* fusion were identified. Patients with *RET*-rearranged lung cancers were frequently female (n=17, 68%) with a median age of 59 (38–84) years and stage 4 disease (n=20, 80%). Patients with *ROS1*-rearranged lung cancers were also frequently female (n=11, 65%) with a median age of 61 (38–89) and stage 4 disease (n=12, 76%).

Thirty-one patients with adenocarcinomas harboring an *EGFR* mutation were selected from a separate institutional database to be used as a control group. Patients with *EGFR*-mutant lung cancers were frequently female (n=21, 68%) with a median age of 61 (36–87) and stage 4 disease 24 (77%). There were no differences in age, sex, or tumor stage between RET- and ROS1-rearranged, and EGFR-mutant lung cancers (Table 1).

### 3.2 Imaging Findings

**3.2.1. Radiologic features/characteristics of RET- and ROS1-rearranged lung cancers—***RET*-rearranged lung cancers were found to be more peripheral in location (n=14, 56%, 95%CI: 35–76%). The primary tumor was solid in density (n=25, 100%, 95%CI: 86–100%) and spiculated in contour (n=13, 54%, 95%CI: 33–74%). It was unlikely to present with cavitation (n=1, 4%, 95%CI: 0.1–20%) or calcification (n=0, 0%, 95%CI: 0–14%). Additional findings included associated lymphadenopathy (n=18, 72%, 95%CI: 51–88%). The *RET*-rearrangement was unlikely to present with effusion (n=10, 40%, 95%CI: 21–61%), lung metastases (n=6, 24%, 95%CI: 9–45%), or extrathoracic disease (n=10, 40%, 95%CI: 21–61%) (Table 2).

*ROS1*-rearranged lung cancers were also found to be more peripheral in location (n=11, 65%, 95%CI: 38- 86%). The primary tumor was solid in density (n=15, 88%, 95%CI: 64–99%) and spiculated in contour (n=12, 71%, 95%CI: 44–90%). It was unlikely to present with cavitation (n=2, 12%, 95%CI: 1–36%) or calcification (n=2, 12%, 95%CI: 1–36%)). Additional findings included often presence of lymphadenopathy (n=10, 59%, 95%CI: 33–

Author Manuscript Author Manuscript Author Manuscript Author Manuscript

82%). The *RET*-rearrangement was unlikely to present with effusion (n=4, 24%, 95%CI: 7–50%), lung metastases (n=4, 24%, 95%CI: 7–50%), or extrathoracic disease (n=3, 18%, 95%CI: 4–43%) (Table 2).

**3.2.2 Comparison with EGFR-mutant lung cancers—**Patients with the *ROS1* fusions were significantly more likely to have more peripheral tumors than patients with *EGFR* mutations (65% vs 32%, P=0.04). In terms of primary tumor characteristics, *RET*- and *ROS1*-rearranged and *EGFR*-mutant lung cancers were most commonly spiculated, solid, and unlikely to contain cavitations or calcifications (Table 2). There was no difference in the axial length and wide of the primary tumors between the three subtypes (*EGFR*-mutant median axial diameter 4.4 × 2.8 cm, *RET*-rearranged median axial diameter 3.8 × 2.6 cm, and *ROS1*-rearranged median axial diameter 4.0 × 2.9 cm) (Table 2).

There was no significant difference in adenopathy between *EGFR*-mutant and *RET*- or *ROS1*-rearranged lung cancers (Table 2). There were likewise no significant differences between groups with respect to the presence of pleural effusion, lung metastasis, or extrathoracic disease (Table 2).

## 4. Discussion

Paradigms for the diagnosis and treatment of non-small cell lung cancer (NSCLC) have developed rapidly over the last decade. Many genomic alterations have been discovered via comprehensive molecular profiling, resulting in improved patient outcomes with appropriate targeted therapy. [10] [11] [12] Adenocarcinomas harboring recurrent gene rearrangements involving *RET* and *ROS1* represent a distinct molecular subset of non-small cell lung cancers.

While *RET* and *ROS1* comprise 1–2% of all lung adenocarcinomas, respectively, [5, 13] it is crucial to identify these patients who could potentially benefit from targeted therapy. Crizotinib has demonstrated marked anti-tumor activity in patients whose tumors harbor *ROS1* fusions. In a phase 1 expansion cohort of 50 patients with advanced *ROS1*-rearranged NSCLC treated with crizotinib, the objective response rate was 72%, with a median duration of response of 18 months and a median progression-free survival of 19 months. [14] In vitro, cabozantinib, has been shown to overcome crizotinib resistance in tumors harboring *ROS1* fusions and several other ROS1 inhibitors are currently in clinical development [15]. *RET*-rearranged lung cancers are sensitive to RET tyrosine kinase inhibition in vitro and in vivo, and a response rate of 38% with cabozantinib has been reported in the first stage of on an ongoing Simon two-stage phase 2 trial. [16] Trials with other RET inhibitors such as ponatinib, lenvatinib, and vandetanib are ongoing.

*RET*- and *ROS1*-rearranged lung cancers share many clinical features include young age at diagnosis and a history of never or former light smoking. [17] From a pathologic perspective, *RET* and *ROS1* fusions likewise share identifiable cytomorphologic features including the presence of extracelluar mucin, cribriform structures, signet ring cells, and hepatoid cytology.[5] In addition, tumors with *RET* rearrangements are more likely to be smaller (< 3cm) and solid in histological morphology when compared to tumors with *EGFR*,

Author Manuscript Author Manuscript Author Manuscript Author Manuscript

*KRAS*, *HER2*, and *BRAF* mutations, or *ALK* fusions. [18] Mukhopadhyay et al provide a brief description of 5 patients with *RET*-rearranged lung adenocarcinomas in whom 4 had lymphangitic carcinomatosis and 3 had multiple bilateral lung nodules. [16] However, to our knowledge, there has not been a systematic radiographic description of these two genomic alterations.

Traditionally, radiology has focused on correlating imaging features and histopathological findings. However there is increasing interest in defining the relationship between radiological findings and specific molecular markers, so called radiogenomics. The practice of using radiological data to predict genomic features of tumors has grown in parallel with the expansion in clinicopathologic genomic profiling and the use of targeted therapy.

There have been many descriptive evaluations of the imaging features of tumors with particular genetic features. [7, 8, 19] In addition, there are a growing number of papers which rely on the extraction of a very large volume of quantitative and qualitative radiological features from an image, with subsequent correlation to gene expression profiles. [20–25] It has also been suggested that radiogenomic analysis can be used to identify genetic subtypes of tumors likely to respond to therapy. [26]

With regard to lung cancer, several studies have investigated the imaging features associated with specific genomic alterations. *ALK*-rearranged lung adenocarcinomas have been associated with a solid tumor appearance, bulky multi-focal lymphadenopathy, and lymphangitic metastasis. [7, 8] There have been mixed results in studies assessing the imaging characteristics of lung adenocarcinomas with *EGFR* mutations. For example, some authors have found *EGFR* –mutant tumors to be most frequently solid, without any significant difference in tumor morphology between *EGFR*-mutant and wild-type tumors [27] or between *EGFR*- and *KRAS*-mutant tumors [28]. Other authors, however, have suggested an association between the size of a lesions ground glass component and the likelihood of an *EGFR* mutation [29]. While Yano et al found no statistical difference between tumors with an *EGFR* mutation and those with *EGFR* wild type, in their series, *EGFR*-mutant tumors were most frequently found in tumors with a GGO ratio > 50% [29]. Lee et al compared the imaging characteristics of subtypes of *EGFR* mutations and found that GGO volume was higher in lesions with exon 21 missense mutation than in wild type tumors. In addition, the prevalence of exon 21 mutation increased along with increasing volume of GGO in a given lesion [19].To our knowledge, this is the first study to describe the CT features of tumors harboring *RET*- and *ROS1* rearranged lung adenocarcinomas. The results of our study demonstrate that adenocarcinoma harboring *RET* and *ROS1* fusions were frequently solid and spiculated. As compared to tumors with *EGFR* mutations, tumors with *ROS1* fusions were more likely to be peripheral in location.

This study was limited in regards to small sample size and retrospective nature. Although study patients were not formally matched, there was no significant difference between the control group and study groups in regards to sex, age or stage of disease. The control group was chosen to be composed as a cohort of adenocarcinomas with the EGFR mutation given the similarity in clinical patient characteristics to adenocarcinoma harboring the RET and ROS1 fusions such as a never smoker status.

Author Manuscript Author Manuscript Author Manuscript Author Manuscript

Lung adenocarcinomas with RET and ROS1 fusions share many radiographic features. In our small study we present the possible radiologic feature of *ROS1* as being more peripheral in location in comparison to *EGFR*-mutant lung cancers. While multiplex comprehensive molecular profiling is advocated for all patients with advanced lung cancers, clinicians **should consider further testing for *RET* and *ROS1* fusions in the presence of these characteristics in lung adenocarcinomas that previously tested negative for *EGFR* mutations or *ALK* rearrangements on non-multiplex testing**. Give the small incidence of these genetic aberrations in lung adenocarcinoma, larger multicenter trials are needed to further elucidate these radiologic features.

## Acknowledgments

We acknowledge the support of the MSKCC Biostatistics Core (P30 CA008748)

## References

1. American Cancer Society. Lung Cancer (Non-Small Cell). 2015. 3/4/2015 [cited 2015 4/11/2015]; Available from: http://www.cancer.org/acs/groups/cid/documents/webcontent/003115-pdf.pdf
2. Lynch TJ, Bell DW, Sordella R, et al. Activating mutations in the epidermal growth factor receptor underlying responsiveness of non-small-cell lung cancer to gefitinib. N Engl J Med. 2004; 350(21): 2129–2139. [PubMed: 15118073]
3. Paez JG, Janne PA, Lee JC, et al. EGFR mutations in lung cancer: correlation with clinical response to gefitinib therapy. Science. 2004; 304(5676):1497–1500. [PubMed: 15118125]
4. Pao W, Miller V, Zakowski M, et al. EGF receptor gene mutations are common in lung cancers from "never smokers" and are associated with sensitivity of tumors to gefitinib and erlotinib. Proc Natl Acad Sci U S A. 2004; 101(36):13306–13311. [PubMed: 15329413]
5. Pan Y, Zhang Y, Li Y, et al. ALK, ROS1 and RET fusions in 1139 lung adenocarcinomas: a comprehensive study of common and fusion pattern-specific clinicopathologic, histologic and cytologic features. Lung Cancer. 2014; 84(2):121–126. [PubMed: 24629636]
6. Lee SE, Lee B, Hong M, et al. Comprehensive analysis of RET and ROS1 rearrangement in lung adenocarcinoma. Mod Pathol. 2015; 28(4):468–479. [PubMed: 25234288]
7. Choi CM, Kim MY, Hwang HJ, et al. Advanced Adenocarcinoma of the Lung: Comparison of CT Characteristics of Patients with Anaplastic Lymphoma Kinase Gene Rearrangement and Those with Epidermal Growth Factor Receptor Mutation. Radiology. 2015:140848.
8. Halpenny DF, Riely GJ, Hayes S, et al. Are there imaging characteristics associated with lung adenocarcinomas harboring ALK rearrangements? Lung Cancer. 2014; 86(2):190–194. [PubMed: 25312988]
9. McErlean A, Panicek DM, Zabor EC, et al. Intra- and interobserver variability in CT measurements in oncology. Radiology. 2013; 269(2):451–459. [PubMed: 23824993]
10. Cufer T, Ovcaricek T, O'Brien ME. Systemic therapy of advanced non-small cell lung cancer: major-developments of the last 5-years. Eur J Cancer. 2013; 49(6):1216–1225. [PubMed: 23265700]
11. Spigel DR, Lin M, O'Neill V, et al. Final survival and safety results from a multicenter, openlabel, phase 3b trial of erlotinib in patients with advanced nonsmall cell lung cancer. Cancer. 2008; 112(12):2749–2755. [PubMed: 18438878]
12. Shaw AT, Kim DW, Nakagawa K, et al. Crizotinib versus chemotherapy in advanced ALKpositive lung cancer. N Engl J Med. 2013; 368(25):2385–2394. [PubMed: 23724913]
13. Bergethon K, Shaw AT, Ou SH, et al. ROS1 rearrangements define a unique molecular class of lung cancers. J Clin Oncol. 2012; 30(8):863–870. [PubMed: 22215748]
14. Shaw AT, Ou SH, Bang YJ, et al. Crizotinib in ROS1-rearranged non-small-cell lung cancer. N Engl J Med. 2014; 371(21):1963–1971. [PubMed: 25264305]

Author Manuscript Author Manuscript Author Manuscript Author Manuscript

15. Katayama R, Kobayashi Y, Friboulet L, et al. Cabozantinib overcomes crizotinib resistance in ROS1 fusion-positive cancer. Clin Cancer Res. 2015; 21(1):166–174. [PubMed: 25351743]
16. Mukhopadhyay S, Pennell NA, Ali SM, et al. RET-Rearranged Lung Adenocarcinomas with Lymphangitic Spread, Psammoma Bodies, and Clinical Responses to Cabozantinib. J Thorac Oncol. 2014; 9(11):1714–1719. [PubMed: 25436805]
17. Takeuchi K, Soda M, Togashi Y, et al. RET, ROS1 and ALK fusions in lung cancer. Nat Med. 2012; 18(3):378–381. [PubMed: 22327623]
18. Wang R, Hu H, Pan Y, et al. RET fusions define a unique molecular and clinicopathologic subtype of non-small-cell lung cancer. J Clin Oncol. 2012; 30(35):4352–4359. [PubMed: 23150706]
19. Lee HJ, Kim YT, Kang CH, et al. Epidermal growth factor receptor mutation in lung adenocarcinomas: relationship with CT characteristics and histologic subtypes. Radiology. 2013; 268(1):254–264. [PubMed: 23468578]
20. Diehn M, Nardini C, Wang DS, et al. Identification of noninvasive imaging surrogates for brain tumor gene-expression modules. Proc Natl Acad Sci U S A. 2008; 105(13):5213–5218. [PubMed: 18362333]
21. Jamshidi N, Diehn M, Bredel M, et al. Illuminating radiogenomic characteristics of glioblastoma multiforme through integration of MR imaging, messenger RNA expression, and DNA copy number variation. Radiology. 2014; 270(1):1–2. [PubMed: 24056404]
22. Karlo CA, Di Paolo PL, Chaim J, et al. Radiogenomics of clear cell renal cell carcinoma: associations between CT imaging features and mutations. Radiology. 2014; 270(2):464–471. [PubMed: 24029645]
23. Nair VS, Gevaert O, Davidzon G, et al. NF-kappaB protein expression associates with (18)F-FDG PET tumor uptake in non-small cell lung cancer: a radiogenomics validation study to understand tumor metabolism. Lung Cancer. 2014; 83(2):189–196. [PubMed: 24355259]
24. Yamamoto S, Maki DD, Korn RL, et al. Radiogenomic analysis of breast cancer using MRI: a preliminary study to define the landscape. AJR Am J Roentgenol. 2012; 199(3):654–663. [PubMed: 22915408]
25. Zinn PO, Mahajan B, Sathyan P, et al. Radiogenomic mapping of edema/cellular invasion MRI-phenotypes in glioblastoma multiforme. PLoS One. 2011; 6(10):e25451. [PubMed: 21998659]
26. Kuo MD, Gollub J, Sirlin CB, et al. Radiogenomic analysis to identify imaging phenotypes associated with drug response gene expression programs in hepatocellular carcinoma. J Vasc Interv Radiol. 2007; 18(7):821–831. [PubMed: 17609439]
27. Hsu JS, Huang MS, Chen CY, et al. Correlation between EGFR mutation status and computed tomography features in patients with advanced pulmonary adenocarcinoma. J Thorac Imaging. 2014; 29(6):357–363. [PubMed: 25303964]
28. Glynn C, Zakowski MF, Ginsberg MS. Are there imaging characteristics associated with epidermal growth factor receptor and KRAS mutations in patients with adenocarcinoma of the lung with bronchioloalveolar features? J Thorac Oncol. 2010; 5(3):344–348. [PubMed: 20087229]
29. Yano M, Sasaki H, Kobayashi Y, et al. Epidermal growth factor receptor gene mutation and computed tomographic findings in peripheral pulmonary adenocarcinoma. J Thorac Oncol. 2006; 1(5):413–416. [PubMed: 17409892]

Author Manuscript Author Manuscript Author Manuscript Author Manuscript

## Highlights

- Radiogenomics can try to characterize the appearance of different lung cancers
- Lung adenocarcinomas with RET and ROS1 fusions share many radiographic features
- ROS1 tumors present as more peripheral lesions
- Genetic testing in lung adenocarcinoma can offer additional targeted treatment

Author Manuscript Author Manuscript Author Manuscript Author Manuscript

**Figure 1.**
Coned down view of an axial CT. 57 year old female with a right lower lobe adenocarcinoma demonstrating peripheral location, solid in nature and spiculated margins. Genomic profiling revealed a *RET* fusion.

Author Manuscript Author Manuscript Author Manuscript Author Manuscript

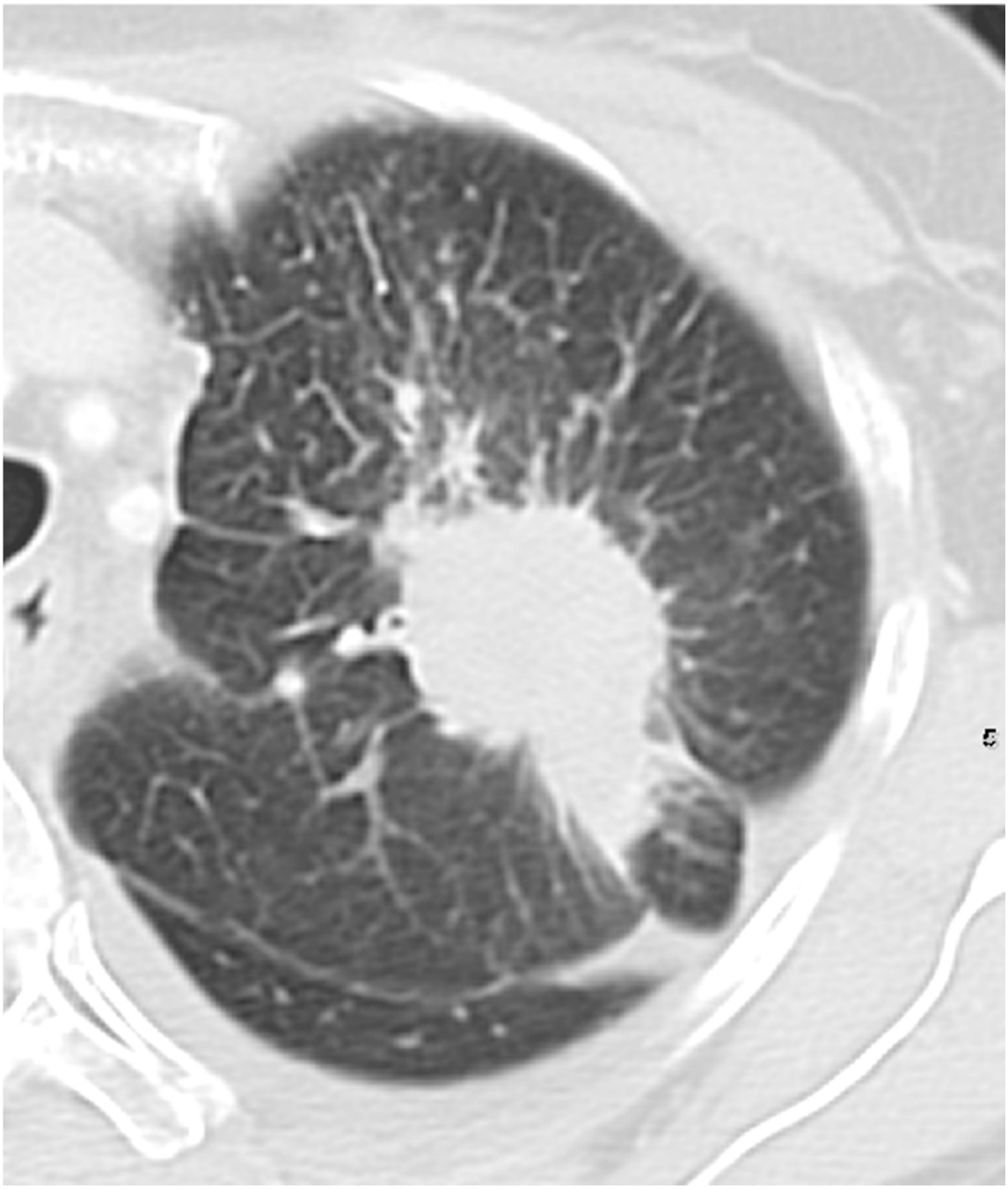

**Figure 2.**
Coned down view of an axial CT. 63 year old female with a left upper lobe adenocarcinoma demonstrating peripheral location, solid in nature and spiculated margins. Genomic profiling revealed a *ROS1* fusion.

Author Manuscript Author Manuscript Author Manuscript Author Manuscript



**Table 1**

Patient Characteristics of EGFR, RET and ROS1

| | All (n=73) | EGFR (n=31) | RET (n=25) | ROS1 (n=17) | p Value | |
|---|---|---|---|---|---|---|
| | | | | | EGFR vs RET/ROS1 | RET vs ROS1 |
| **Age (years), median (range)** | 61 (36, 89) | 61 (36, 87) | 59 (38, 84) | 61 (38, 89) | 0.80 | 0.58 |
| **Gender, n(%)** | | | | | | |
| F | 49 (67%) | 21 (68%) | 17 (68%) | 11 (65%) | 0.99 | 0.99 |
| M | 24 (33%) | 10 (32%) | 8 (32%) | 6 (35%) | | |
| **Stage, n(%)** | | | | | | |
| 1 | 1 (1%) | 0 (0%) | 1 (4%) | 0 (0%) | 0.95 | 0.90 |
| 2 | 5 (7%) | 2 (6%) | 2 (8%) | 1 (6%) | 0.99 (1 vs 2–4) | 0.99 (1 vs 2–4) |
| 3 | 10 (14%) | 5 (16%) | 2 (8%) | 3 (18%) | | |
| 4 | 57 (78%) | 24 (77%) | 20 (80%) | 13 (76%) | | |

*Lung Cancer*. Author manuscript; available in PMC 2016 November 01.

Author Manuscript Author Manuscript Author Manuscript Author Manuscript



**Table 2**

CT features of EGFR, RET and ROS1

| | | EGFR (n=31) | RET (n=25) | ROS1 (n=17) | Fisher's Exact Test p-Value | |
|---|---|---|---|---|---|---|
| | | n (%) | n (%) | n (%) | EGFR vs RET | EGFR vs ROS1 |
| **Central or Peripheral** | Central | 21 (68%) | 11 (44%) | 6 (35%) | 0.11 | 0.04 |
| | Peripheral | 10 (32%) | 14 (56%) | 11 (65%) | | |
| **Cavitation in primary tumor** | no | 31 (100%) | 24 (96%) | 15 (88%) | 0.45 | 0.12 |
| | yes | 0 (0%) | 1 (4%) | 2 (12%) | | |
| **Calcification in primary tumor** | no | 31 (100%) | 25 (100%) | 16 (94%) | NA | 0.35 |
| | yes | 0 (0%) | 0 (0%) | 1 (6%) | | |
| **Solid density of primary tumor** | no | 4 (13%) | 0 (0%) | 2 (12%) | 0.12 | 0.99 |
| | yes | 27 (87%) | 25 (100%) | 15 (88%) | | |
| **Ground Glass of primary tumor** | no | 30 (97%) | 25 (100%) | 17 (100%) | 0.99 | 0.99 |
| | yes | 1 (3%) | 0 (0%) | 0 (0%) | | |
| **Mixed Solid/Ground Glass** | no | 30 (97%) | 25 (100%) | 15 (88%) | 0.99 | 0.28 |
| | yes | 1 (3%) | 0 (0%) | 2 (12%) | | |
| **Air Bronchogram within the tumor** | no | 29 (94%) | 23 (92%) | 16 (94%) | 0.99 | 0.99 |
| | yes | 2 (6%) | 2 (8%) | 1 (6%) | | |
| **Lymphadenopathy** | no | 11 (35%) | 7 (28%) | 7 (41%) | 0.58 | 0.76 |
| | yes | 20 (65%) | 18 (72%) | 10 (59%) | | |
| **Count of Adenopathy** | 0 | 11 (35%) | 7 (28%) | 8 (47%) | 0.85 | 0.62 |
| | 1 | 3 (10%) | 2 (8%) | 2 (12%) | | |
| | >1 | 17 (55%) | 16 (64%) | 7 (41%) | | |
| **Volume of Adenopathy** | 0–1 | 11 (35%) | 7 (28%) | 8 (47%) | 0.27 | 0.46 |
| | 1–1.5cm | 12 (39%) | 6 (24%) | 4 (24%) | | |
| | 1.5–3cm | 6 (19%) | 11 (44%) | 2 (12%) | | |
| | >3.0cm | 2 (6%) | 1 (4%) | 3 (18%) | | |

*Lung Cancer*. Author manuscript; available in PMC 2016 November 01.

Author Manuscript Author Manuscript Author Manuscript Author Manuscript

| | | | EGFR (n=31) | RET (n=25) | ROS1 (n=17) | Fisher's Exact Test p-Value | |
|---|---|---|---|---|---|---|---|
| | | | n (%) | n (%) | n (%) | EGFR vs RET | EGFR vs ROS1 |
| **Effusion** | | no | 18 (58%) | 15 (60%) | 13 (76%) | 0.99 | 0.34 |
| | | yes | 13 (42%) | 10 (40%) | 4 (24%) | | |
| **Lung Metastases** | | no | 17 (55%) | 19 (76%) | 13 (76%) | 0.16 | 0.21 |
| | | yes | 14 (45%) | 6 (24%) | 4 (24%) | | |
| **Extrathoracic Disease** | | no | 18 (58%) | 15 (60%) | 14 (82%) | 0.99 | 0.12 |
| | | yes | 13 (42%) | 10 (40%) | 3 (18%) | | |
| **Contour** | | round | 1 (4%) | 0 (0%) | 0 (0%) | 0.96 | 0.61 |
| | | lobulated | 4 (15%) | 5 (21%) | 1 (6%) | | |
| | | spiculated | 14 (52%) | 13 (54%) | 12 (71%) | | |
| | | consolidation | 8 (30%) | 6 (25%) | 4 (24%) | | |
| | | | Median (Range) | Median (Range) | Median (Range) | Wilcoxon rank-sum Test p-Value | |
| | | | | | | EGFR vs RET | EGFR vs ROS1 |
| **Mass Axial Length** | | | 4.4 (1.2, 10.8) | 3.8 (1.5, 8.7) | 4.0 (1.5, 9.8) | 0.54 | 0.52 |
| **Mass Axial Width** | | | 2.8 (1.2, 8.5) | 2.6 (1.1, 7.2) | 2.9 (1.4, 5.7) | 0.61 | 0.55 |